

Structure of calcium tetrasodium bis-cyclotriphosphate $\text{CaNa}_4(\text{P}_3\text{O}_9)_2$ by X-ray diffraction and solid-state NMR

Isaac Abrahams,^{*a} Geoffery E. Hawkes,^a A. Ahmed,^{†a} Katrin Franks,^b Jonathan C. Knowles,^b Philippe R. Bodart^{‡c} and Teresa Nunes^c

^a Structural Chemistry Group, Department of Chemistry, Queen Mary, University of London, Mile End Road, London, UK E1 4NS. E-mail: i.abrahams@qmul.ac.uk

^b Department of Biomaterials, Eastman Dental Institute, University of London, Gray's Inn Road, London, UK WC1X 8LD

^c ICTPOLIIST, Departamento de Engenharia de Materiais, Av. Rovisco Pais, 1096 Lisboa Codex, Portugal

Received 4th October 2001, Accepted 25th January 2002
First published as an Advance Article on the web 15th March 2002

The crystal structure of $\text{CaNa}_4(\text{P}_3\text{O}_9)_2$ has been determined using single crystal X-ray diffraction. The ^{23}Na and ^{31}P magic angle spinning solid-state NMR data are consistent with the centrosymmetric space group assignment of $C2/c$ and the cation distribution of two distinct sodium sites. The structure determination confirms the presence of the cyclic triphosphate unit as opposed to a cyclic hexaphosphate or metaphosphate chains. Phosphorus and sodium edge EXAFS data are discussed with respect to the structure.

Introduction

We have been investigating phosphate based glasses, glass ceramics and ceramics as materials suitable for bone replacement in hard tissue surgery and periodontology.^{1,2} As part of this work we have attempted to correlate the structures observed in glasses, with those of the crystallised glass ceramics of the same composition. The principal glasses under study are in the $\text{Na}_2\text{O} : \text{CaO} : \text{P}_2\text{O}_5$ system. On crystallisation of glasses in this system two crystallographically distinct calcium sodium metaphosphates are observed *viz.* $\text{CaNa}(\text{PO}_3)_3$ and $\text{CaNa}_4(\text{PO}_3)_6$.³ The structure of the former has been found to consist of linear metaphosphate chains,⁴ while the structure of the latter was proposed by Griffith⁵ as early as 1962 to consist of cyclic triphosphate ions, however until now no definitive crystal structure information has been obtained. Solid-state NMR is unable to distinguish between Q^2 phosphorus atoms in rings or chains or indeed if the structure comprises of a hexaphosphate ring. The purpose of this study is to fully characterise the structure of $\text{CaNa}_4(\text{PO}_3)_6$ using X-ray diffraction, EXAFS and solid-state MAS NMR.

Experimental

Preparation

The title compound was prepared as a polycrystalline powder by crystallising a glass of the stoichiometric composition. Na_2CO_3 , $\text{NH}_4\text{H}_2\text{PO}_4$ and CaO were ground together as a slurry in ethanol. After drying, the powder was heated for 1 hour at 1000 °C until molten. The molten glass was poured into a hot graphite mould at 350 °C and allowed to cool slowly to room temperature in a furnace. The cooled glass was then reheated to

600 °C to facilitate crystallisation, and the ceramic produced ground to a fine powder after cooling. Found: Na 15.46 (flame photometry); Ca 6.13% (EDTA titration). Calc. for $\text{CaNa}_4\text{-P}_6\text{O}_{18}$: Na 15.18, Ca 6.67%. Single crystals were prepared by exponential slow cooling of the melt in the furnace over a period of 12 h.

X-Ray crystallography

Single crystal X-ray diffraction data were collected on the title compound. Intensity data were collected on an Enraf-Nonius CAD-4 diffractometer using $\text{Mo-K}\alpha$ radiation ($\lambda = 0.71073 \text{ \AA}$) with ω - 2θ scans at 293(2) K. Systematic absences in the data were consistent with the monoclinic space groups, Cc and $C2/c$. Solution and refinement proceeded in the centrosymmetric space group as suggested by the solid-state NMR results (see Results and discussion). The structure was solved by direct methods using SHELXS-97⁶ and developed by difference Fourier techniques with subsequent refinement on F^2 by full matrix least squares using SHELXL-97.⁶ In the final stages of refinement, data were corrected for absorption against a refined isotropic model with the program DIFABS.⁷ Anisotropic thermal parameters were refined for all atoms. Graphics were obtained using ORTEP-3⁸ and WinGX⁹ was used to prepare material for publication. Crystal and refinement parameters for $\text{CaNa}_4(\text{P}_3\text{O}_9)_2$ are summarised in Table 1.

The absence of crystalline impurities was confirmed by X-ray powder diffraction, with data collected on a Siemens D5000 diffractometer in flat plate mode using graphite monochromated $\text{Cu-K}\alpha$ radiation ($\lambda = 1.5418 \text{ \AA}$). Data were collected in the range 5–110° 2θ , in steps of 0.02° with a scan time of 12 s per step. The observed peaks in the X-ray powder diffraction pattern were consistent with those reported by Grenier *et al.*³ Reitveld analysis of the powder diffraction data, using the program GSAS,¹⁰ confirmed the determined single crystal structure.

CCDC reference number 172172.

See <http://www.rsc.org/suppdata/dt/b1/b109036b/> for crystallographic data in CIF or other electronic format.

[†] Present address, Department of Chemistry, University of Southampton, Highfield, Southampton, UK SO17 1BJ.

[‡] Present address: Laboratoire de Dynamique et Structure des Matériaux Moléculaires, Université des Sciences et Technologies de Lille, 59655 Villeneuve d'Ascq Cedex, France.

Table 1 Crystal and structure refinement data for $\text{CaNa}_4(\text{P}_3\text{O}_9)_2$

Empirical formula	$\text{CaNa}_4\text{P}_6\text{O}_{18}$
<i>M</i>	605.86
<i>T/K</i>	293(2)
Crystal system	Monoclinic
Space group	<i>C2/c</i>
<i>a/Å</i>	13.069(2)
<i>b/Å</i>	8.054(2)
<i>c/Å</i>	14.164(3)
$\beta/^\circ$	94.60(2)
<i>U/Å</i>	1486.1(5)
<i>Z</i>	4
$\mu(\text{Mo-K}\alpha)/\text{mm}^{-1}$	1.292
Reflections collected	1466
Independent reflections	1300
<i>R</i> _{int}	0.0564
Final <i>R1</i> , <i>wR2</i> [<i>I</i> > 2σ(<i>I</i>)]	0.0455, 0.1265
Final <i>R1</i> , <i>wR2</i> [all data]	0.0631, 0.1340

NMR spectroscopy

Single-pulse ^{23}Na and ^{31}P spectra were measured at 158.7 and 242.9 MHz respectively using a Bruker AMX-600 spectrometer. The sample was contained in a 4 mm o.d. rotor and magic angle spinning (MAS) was employed at 12 kHz. 16 transients were acquired for each of the ^{31}P and ^{23}Na spectra, with a recycle delay of 60 s for ^{31}P and 8 s for ^{23}Na . Spectra were referenced ($\delta_{\text{cs}} = 0.0$) against solutions of 85% H_3PO_4 and 0.1 M NaCl for the ^{31}P and ^{23}Na spectra respectively. The ^{23}Na MAS NMR spectrum was simulated using the program QUASAR.¹¹ The overlapping lines in the ^{31}P MAS NMR spectrum were deconvoluted using the Bruker WINFIT software,¹² and the ^{31}P shielding tensor components were determined from these line intensities with the Bruker WIN-MAS program.¹³

EXAFS

EXAFS data were collected on the soft X-ray station, 3.4, at the CLRC Daresbury Synchrotron Radiation Source. Fluorescence data were collected at the P and Na edges. Samples were mounted as graphite impregnated pellets (13 mm diameter). Pairs of plane Ge(111) and Beryl crystal monochromators were used for the P and Na data collections respectively. Scans were collected between 2120–2500 eV and 1040–1300 eV for the P and Na data respectively, with a summation of three and four scans respectively to give an improved signal to noise ratio. Data were processed in the conventional manner using the Daresbury suite of programs EXCALIB, EXBACK and EXCURV92.¹⁴ Fourier filtering was carried out to include the regions 0.5–3.5 and 1–4 Å of the Fourier transform for P and Na data respectively. This allowed for refinement of the radial distances (RD) and Debye–Waller type factors, *A*, ($=2\sigma^2$) for the first four coordination shells around the excited atoms in each case. The goodness of fit was measured by an *R*-factor,¹⁴ with the errors in RD $\approx \pm 0.02$ Å and *A* $\approx \pm 20\%$. Average coordination numbers were determined from the crystal structure.

Results and discussion

Significant contact distances and angles in $\text{CaNa}_4(\text{P}_3\text{O}_9)_2$ are given in Table 2. The structure of $\text{CaNa}_4(\text{P}_3\text{O}_9)_2$ (Fig. 1) consists of cyclic triphosphate ions bridged by Na^+ and Ca^{2+} ions and confirms the structural formula of $\text{CaNa}_4(\text{P}_3\text{O}_9)_2$. Three crystallographically distinct P atoms are present, each with two longer bonds to bridging oxygens (ave. 1.61 Å) and two shorter bonds to terminal oxygens (ave. 1.48 Å). The terminal oxygens have ionic contacts to Na^+ and/or Ca^{2+} ions.

The calcium ions sit in octahedral holes in the lattice where they link six (P_3O_9) units. The ionic contacts between the terminal oxygens and the Ca^{2+} ions are within the sum of the ionic radii for these ions, with an average contact distance of 2.36 Å.

Table 2 Selected bond lengths, significant contact distances (Å) and angles ($^\circ$) for $\text{CaNa}_4(\text{P}_3\text{O}_9)_2$

Ca(1)–O(1)	2.341(3) × 2	Ca(1)–O(8)	2.354(3) × 2
Ca(1)–O(5)	2.377(3) × 2	Na(1)–O(2)	2.336(4)
Na(1)–O(8)	2.409(4)	Na(1)–O(9)	2.543(4)
Na(1)–O(6)	2.640(5)	Na(1)–O(2')	2.670(4)
Na(2)–O(2)	2.398(4)	Na(2)–O(1)	2.412(4)
Na(2)–O(9)	2.420(4)	Na(2)–O(9')	2.423(4)
Na(2)–O(5)	2.482(4)	Na(2)–O(6)	2.505(4)
P(1)–O(2)	1.472(3)	P(1)–O(1)	1.484(3)
P(1)–O(4)	1.602(3)	P(1)–O(3)	1.621(3)
P(2)–O(6)	1.462(4)	P(2)–O(5)	1.488(3)
P(2)–O(4)	1.609(4)	P(2)–O(7)	1.609(3)
P(3)–O(9)	1.473(3)	P(3)–O(8)	1.478(3)
P(3)–O(7)	1.606(3)	P(3)–O(3)	1.606(3)
O(1)–P(1)–O(2)	119.7(2)	O(1)–P(1)–O(3)	106.9(2)
O(1)–P(1)–O(4)	107.4(2)	O(2)–P(1)–O(3)	109.7(2)
O(2)–P(1)–O(4)	110.5(2)	O(3)–P(1)–O(4)	100.9(2)
O(4)–P(2)–O(5)	109.3(2)	O(4)–P(2)–O(6)	107.4(2)
O(4)–P(2)–O(7)	101.1(2)	O(5)–P(2)–O(6)	120.4(2)
O(5)–P(2)–O(7)	108.3(2)	O(6)–P(2)–O(7)	108.6(2)
O(3)–P(3)–O(7)	101.3(2)	O(3)–P(3)–O(8)	106.7(2)
O(3)–P(3)–O(9)	110.7(2)	O(7)–P(3)–O(8)	107.2(2)
O(7)–P(3)–O(9)	109.4(2)	O(8)–P(3)–O(9)	119.9(2)
P(1)–O(3)–P(3)	127.4(2)	P(1)–O(4)–P(2)	130.0(2)
P(2)–O(7)–P(3)	129.9(2)		

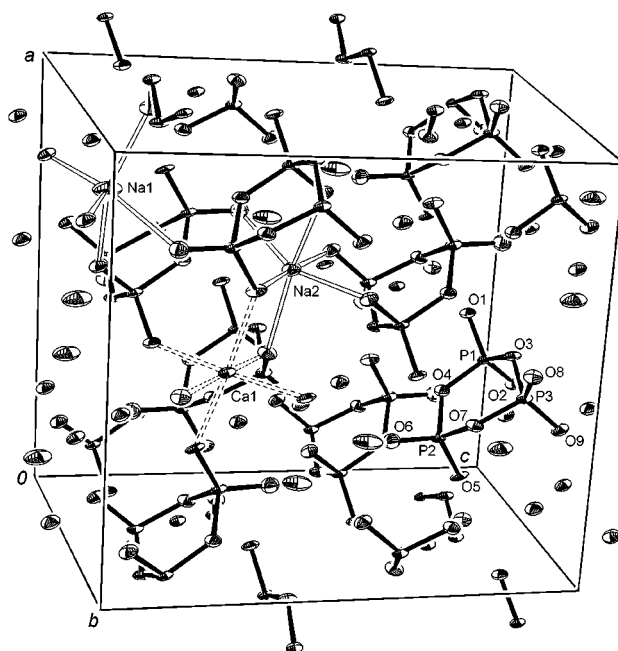


Fig. 1 Unit cell contents of $\text{CaNa}_4(\text{P}_3\text{O}_9)_2$. Thermal ellipsoids are shown (50% probability). Ionic contacts for representative Na^+ (open bonds) and Ca^{2+} (dashed bonds) ions are shown.

The sodium coordinations are significantly more distorted. Na(1) is essentially in a distorted trigonal bipyramidal coordination, with five contacts between 2.34 and 2.67 Å to terminal oxygens on neighboring (P_3O_9) units; the next nearest contact to oxygen is at 2.95 Å. In contrast Na(2) shows a distorted octahedral coordination with six short contacts to terminal oxygens (2.40–2.51 Å), the next nearest contact at 2.99 Å is to O(4) which is a bridging oxygen. The average of the closest contacts (2.52 and 2.44 Å for Na(1) and Na(2) respectively) in both cases lie in the range expected for Na–O of 2.25–2.78 Å.¹⁵

$\text{CaNa}_4(\text{P}_3\text{O}_9)_2$ is essentially isostructural with $(\text{NH}_4)_2\text{Na}_2\text{Hg}(\text{P}_3\text{O}_9)_2$,¹⁶ which is the only other published example of this structure type. A search of the ICSD database¹⁷ revealed 58 crystal structures classified as containing the cyclic triphosphate unit (P_3O_9) with 144 crystallographically distinct PO_4 moieties. The average P–O bridging bond length over all

Table 3 Summary of refined EXAFS parameters for $\text{CaNa}_4(\text{P}_3\text{O}_9)_2$

	Shell	$R/\text{\AA}$	$2\sigma^2/\text{\AA}^2$	$R(\%)$
(a) P data				
Shell 1	4 O	1.51	0.01	28.15
Shell 2	2 P	2.97	0.02	
Shell 3	4 Na	3.55	0.03	
Shell 4	1 Ca	3.53	0.01	
(b) Na data				
Shell 1	4.5 O	2.35	0.04	9.01
Shell 2	1 O	2.70	0.01	
Shell 3	3.5 O	3.02	0.01	
Shell 4	5.5 P	3.73	0.05	

144 tetrahedra examined was 1.612 \AA , while for P–O terminal bonds an average value of 1.477 \AA was calculated. These values are close to those observed in the present study. The average tetrahedral distortion index,¹⁸ D_{ind} , was 37.3 and ranged from 0.6 in $\text{CeP}_3\text{O}_9 \cdot 3\text{H}_2\text{O}$,¹⁹ to 266.2 in YbP_3O_9 ,²⁰ These compare with values in the present work of 31.60, 32.58 and 31.57 for the P(1), P(2) and P(3) tetrahedra respectively. These distortions are also reflected in the P–O–P ring angles, which vary from 127.7–130.0° in $\text{CaNa}_4(\text{P}_3\text{O}_9)_2$.

EXAFS data

The results of the EXAFS refinements are shown in Table 3 and Figs. 2 and 3. A four shell model was fitted to the P-EXAFS data. The first coordination shell of four oxygen atoms constitutes an average of the P–O bonds in the three PO_4 tetrahedra with the second shell formed from two neighbouring P atoms in

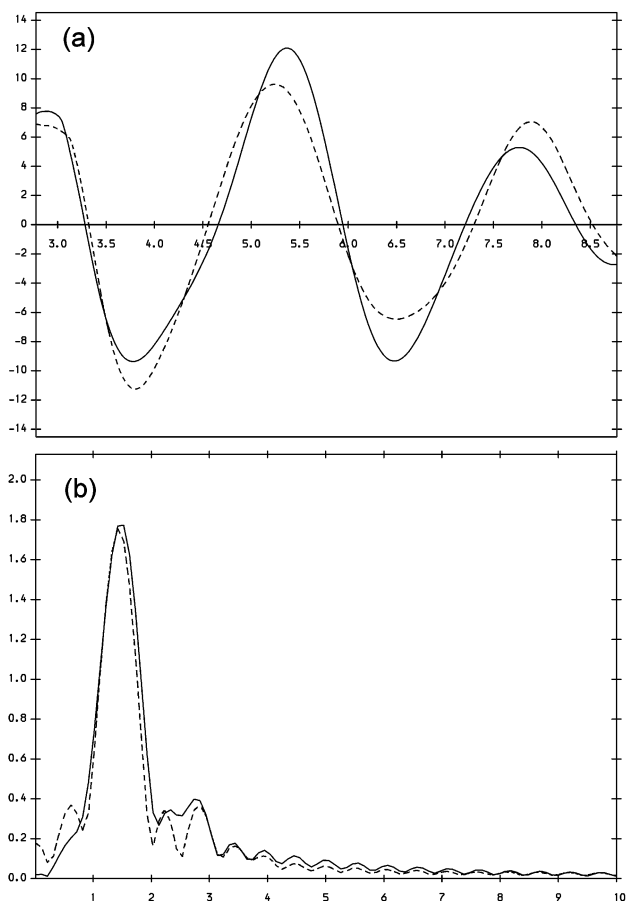


Fig. 2 (a) Refined P-EXAFS spectrum (k^3 weighted) and (b) corresponding Fourier transform for $\text{CaNa}_4(\text{P}_3\text{O}_9)_2$ showing observed (dashed) and calculated lines (solid).

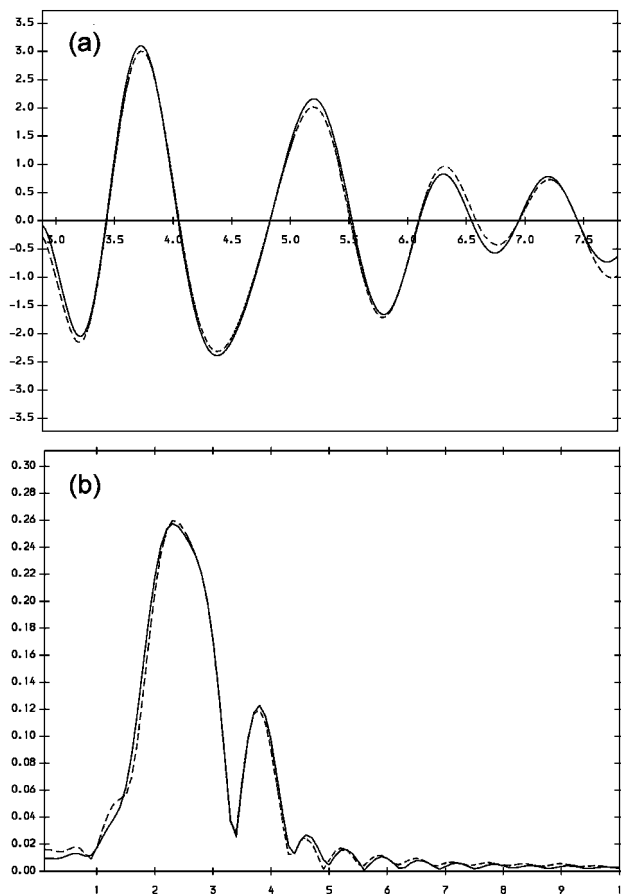


Fig. 3 (a) Refined Na-EXAFS spectrum (k^3 weighted) and (b) corresponding Fourier transform for $\text{CaNa}_4(\text{P}_3\text{O}_9)_2$ showing observed (dashed) and calculated lines (solid).

the (P_3O_9) ring. The third and fourth shells are the next nearest Na^+ and Ca^{2+} ions. The refined radial distances of 1.51, 2.97, 3.55 and 3.53 \AA for the first, second third and fourth shells respectively, compare well with those obtained from an average of contacts in the crystallographic data (1.54, 2.91, 3.49 and 3.51 \AA respectively). Four coordination shells were also fitted to the Na-EXAFS data. From the average contacts in the crystal structure it is evident that three distinct ranges of Na–O contacts are present: 2.34–2.54, 2.64–2.67 and 2.95–3.34 \AA . These were modelled accordingly as the first three shells with the fourth shell being the next nearest P atoms. The refined radial distances of 2.35, 2.70, 3.02 and 3.73 \AA compare reasonably well with average distances in the crystal structure of 2.44, 2.65, 3.12 and 3.58 \AA . The significant difference in the last shell is probably due to the fact that several contacts to Na^+ and Ca^{2+} are evident in the crystal structure around 3.5 \AA , which could not be modelled successfully as further shells with these data. The relatively high Debye–Waller factor on shell 4 reflects this.

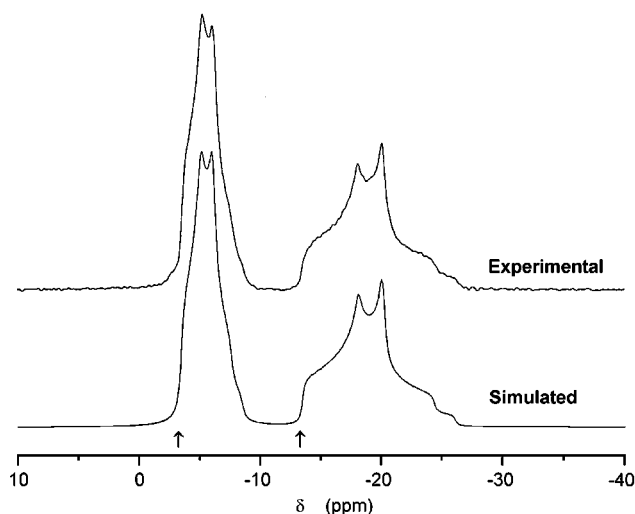
^{23}Na solid-state NMR spectra

The ^{23}Na MAS NMR spectrum of $\text{CaNa}_4(\text{P}_3\text{O}_9)_2$ is shown in Fig. 4 and clearly indicates two principal sodium sites. The result of iterative simulation of the spectrum is also shown in Fig. 4 and gave the parameters listed in Table 4. The derived quadrupole parameters are close to those determined by Koller *et al.*²¹ for the cyclic trimetaphosphate $\text{Na}_3(\text{PO}_3)_3$ viz. two equally populated sites with chemical shifts²² at $\delta +1.5$ and -7.7 with quadrupole coupling constants 1.57 and 2.20 MHz, and asymmetry parameters 0.55 and 0.70 respectively. Also given in Table 4 are the averages for these same quadrupole parameters derived from the ^{23}Na MAS NMR spectra of three Na/Ca/Al/phosphate glass ceramics from an earlier study.¹ In that investigation¹ of the glass ceramics, preliminary evidence

Table 4 ^{23}Na NMR parameters^a for $\text{CaNa}_4(\text{P}_3\text{O}_9)_2$

	δ_{iso}^b	C_q/MHz^c	η_q^d
Site 1 ^e	-3.3 (-1.6)	1.405 ± 0.006 (1.53 ± 0.02)	0.60 ± 0.02 (0.60 ± 0.08)
Site 2 ^e	-13.3 (-10.8)	2.191 ± 0.004 (2.30 ± 0.06)	0.69 ± 0.07 (0.69 ± 0.04)

^a The values in parentheses are the averages for the corresponding parameters found from iterative simulation of the 79.4 MHz ^{23}Na MAS NMR spectra of three Na/Ca/Al/phosphate glass ceramics.⁴ ^b The chemical shifts are referenced to external NaCl solution. ^{c,d} The quadrupole coupling constant and asymmetry parameter respectively. ^e The site populations are equal.

**Fig. 4** Experimental (upper) and simulated (lower) 158.8 MHz ^{23}Na MAS NMR spectra of $\text{CaNa}_4(\text{P}_3\text{O}_9)_2$. The parameters for the simulation are given in Table 4, and the arrows indicate the isotropic chemical shifts.

was presented for the dominant phosphate species being the cyclic trimetaphosphate and it was proposed that this was present as $\text{CaNa}_4(\text{PO}_3)_6$. Overall there is excellent agreement between the ^{23}Na parameters for the authentic material from this study and the ceramics, providing additional evidence for the importance of the cyclic trimetaphosphates in the ceramics.

Koller *et al.*²¹ used the bond valence method, based on the approach of Brown and Altermatt,²³ to calculate a shift parameter (A), and found a linear correlation between A and the ^{23}Na chemical shift δ :

$$\delta = -133.6A + 114.7 \quad (1)$$

The constant term in eqn. (1) has been corrected by +7.1 ppm from that found by Koller *et al.*²¹ in order to accommodate the difference in ^{23}Na reference sample.²³ The shift parameter A is defined as:

$$A = \sum_j (W_i/r_i^n) \quad (2)$$

where W_i is the total atomic valence of the i th oxygen atom, and the summation runs over the j oxygens within a sphere of radius 3.4 Å centred at the sodium atom. The r_i are the sodium–oxygen distances (Å) and the best correlation between A values and experimental isotropic shifts was for $n = 2.87$. The total atomic valence of each oxygen atom, W_i , is given by:

$$W_i = \sum_j s_{ij} \quad (3)$$

where the summation runs over all cations bonded to the oxygen. The oxygen–cation bond valences, s_{ij} , are calculated as:

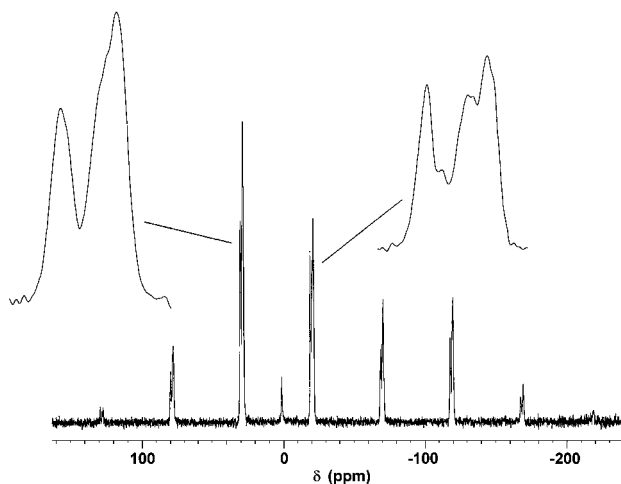
$$s_{ij} = \exp[(r_0 - r_{ij})/B] \quad (4)$$

where r_0 is the empirically derived length of the oxygen–cation bond of unit valence (values are tabulated by Brown and Altermatt)²³ and $B = 0.37$ is a constant. Among the materials used by Koller *et al.*²¹ in establishing the correlation [eqn. (1)] was the cyclic trimetaphosphate $\text{Na}_3\text{P}_3\text{O}_9$, and using the published²⁴ structural data A values of 0.886 and 0.876 were calculated²¹ for the two distinct sodium sites Na(1) and Na(2) respectively. These A values predict [eqn. (1)] ^{23}Na chemical shifts at $\delta -2.9$ and -4.3 , compared with the experimental values^{21,22} $\delta +1.5$ and -7.7 . Using the same structural data²⁴ for $\text{Na}_3\text{P}_3\text{O}_9$ we calculate A values of 0.892 and 0.938 which predict [eqn. (1)] $\delta -4.5$ and -10.6 , in somewhat better agreement with the experiment. This would indicate that (in the nomenclature used by Ondik)²⁴ the resonance due to Na(1) is at higher frequency than that from Na(2) in $\text{Na}_3\text{P}_3\text{O}_9$.

From the X-ray structural data reported here for $\text{CaNa}_4(\text{P}_3\text{O}_9)_2$ we calculate A values of 0.820 and 1.075 for sodium sites Na(1) and Na(2) respectively, which predict ^{23}Na shifts at $\delta 5.1$ and -28.9 (*cf.* $\delta -3.3$ and -13.3 found experimentally, given in Table 4). This correlation between predicted and experimental ^{23}Na shifts is clearly not strong enough to conclusively assign the two resonances, but the indication is that the assignment may be Na(1) at $\delta -3.3$ and Na(2) at $\delta -13.3$. From the crystal structure it is evident that the Na(1) environment is five-coordinate, while the Na(2) environment has six nearest neighbour oxygens in a distorted octahedral environment. It is likely that a more symmetrical environment would result in a lower value for the quadrupole coupling constant, C_q . This suggests that the trigonal bipyramidal coordination of Na(1) ($C_q = 1.405$ MHz) has a higher effective symmetry than the distorted octahedron around Na(2) ($C_q = 2.191$ MHz).

^{31}P solid-state NMR spectra

The ^{31}P MAS NMR spectrum of $\text{CaNa}_4(\text{PO}_3)_6$ is shown in Fig. 5. The centre band is in the region $\delta -18$ to -22 and this is

**Fig. 5** The 242.9 MHz ^{31}P MAS NMR spectrum of $\text{CaNa}_4(\text{P}_3\text{O}_9)_2$ with MAS rate 12 kHz; inset is the expansion of the centre band region and the first (+1) spinning side band.

flanked by the spinning side bands. The singlet at $\delta 1.0$ is due to orthophosphate impurity and constitutes *ca.* 1.6% of the total integrated intensity of the ^{31}P spectrum. The chemical shifts of the six overlapping lines within the centre band were measured after deconvolution of the band (see Experimental) and are given in Table 5, together with their integrals expressed as a percentage of the total centre band intensity. Clearly there are

Table 5 ^{31}P centre band NMR data for $\text{CaNa}_4(\text{P}_3\text{O}_9)_2$

δ^a	$\Delta\nu_{1/2}^b$	Intensity ^c
-19.0	145	26
-19.7	116	7
-20.4	160	21
-20.8	106	9
-21.2	111	15
-21.5	148	22

^a The ^{31}P chemical shifts are referenced to external 85% aqueous phosphoric acid. ^b Full width at half height of the resonances, obtained from deconvolution of the centre band as described in the Experimental section. ^c Relative intensities of the resonances within the centre band only.

three major resonances of comparable intensity at δ -19.0, -20.4 and -21.5, with three lesser resonances at δ -19.7, -20.8 and -21.2. Usually it is necessary to sum the integrals of a particular resonance over the centre band and all the spinning side bands. However for the very closely separated resonances here, only three resonances could be identified in the spinning side bands; this loss of resolution in the side bands in comparison with the centre band cannot be due to slight instability in the MAS rate over the period of the spectral accumulation (16 ms). However the integrals given in Table 5 will be a reasonable measure of the phosphorus site occupancies if the ^{31}P chemical shift tensor components are equal for all resonances. While this is a reasonable assumption to make for these very similar phosphorus environments, it is not possible to confirm this from the available data.

The origin of the additional lines in the centre band is most probably scalar ^{31}P - ^{31}P spin-spin (J) coupling, a homogeneous interaction which is not removed by the sample rotation.²⁵ The solution state ^{31}P NMR spectrum of the cyclic trimetaphosphate system is a singlet,²⁶ but in the solid state where the three phosphorus sites are rendered inequivalent by crystal constraints it is to be expected that multiplet structure will exist due to the two-bond ^{31}P - ^{31}P coupling which will be of the order 17–20 Hz.^{26,27} There has been considerable attention paid to the effect of homonuclear J -coupling on the appearance of MAS NMR spectra, for the limits of both weak²⁸ and strong²⁹ coupling. It is clear²⁸ that there are two effects which complicate the appearance of the spectra in the case of weak coupling. The first of these is that the relative intensities of the lines within a scalar spin-spin coupled multiplet may be distorted with respect to the intensities expected from a corresponding 'solution' spectrum, and the second effect is that the spinning side bands may exhibit 'a conspicuous line shape or broadening'. Both of these effects are most likely evident in this ^{31}P spectrum, but a detailed analysis, following previous work^{28–30} is beyond the scope of this immediate study.

Each side band was analysed by deconvolution as comprising three resonances labelled A, B and C, and for the analysis of the chemical shift tensor components the centre band intensity for resonance A was taken as the sum of the intensities for the resonances at δ -19.0 and -19.7, that for resonance B as the sum of intensities at δ -20.4 and -20.8, and that for resonance C as the sum of the intensities at δ -21.2 and -21.5. The analysis of the side band intensities used the method of Herzfeld and Berger³¹ (see Experimental) and yields the principal components (δ_{11} , δ_{22} , δ_{33}) of the chemical shift tensor, for which the isotropic chemical shift (δ_{iso}) is given by:

$$\delta_{\text{iso}} = (\delta_{11} + \delta_{22} + \delta_{33})/3 \quad (5)$$

These principal elements were ordered according to the Haerberlen convention:³² $|\delta_{33} - \delta_{\text{iso}}| > |\delta_{11} - \delta_{\text{iso}}| > |\delta_{22} - \delta_{\text{iso}}|$. The chemical shift anisotropy ($\Delta\delta$) and asymmetry parameter (η) are given by:

Table 6 ^{31}P chemical shift tensor components for $\text{CaNa}_4(\text{P}_3\text{O}_9)_2$

	%	δ_{iso}	δ_{11}	δ_{22}	δ_{33}	$\Delta\delta$	η
Band A	31	-19.0	72	44	-173	-230	0.18
Band B	31	-20.4	76	38	-176	-233	0.24
Band C	38	-21.5	81	30	-176	-231	0.33

$$\Delta\delta = \delta_{33} - (\delta_{11} + \delta_{22})/2 \quad (6)$$

$$\eta = (\delta_{22} - \delta_{11})/(\delta_{33} - \delta_{\text{iso}}) \quad (7)$$

The data are given in Table 6 for bands A, B and C. The ^{31}P shielding tensor components for the three bands are very similar to each other and average to $\delta_{11} = 76 \pm 5$, $\delta_{22} = 37 \pm 7$, $\delta_{33} = -175 \pm 2$, $\Delta\delta = -231 \pm 2$, and these averages compare closely with those from the corresponding Q^2 band assigned to the cyclic trimetaphosphate species in the earlier¹ study of Na/Ca/Al/phosphate ceramics $\delta_{11} = 85 \pm 11$, $\delta_{22} = 25 \pm 1$, $\delta_{33} = -173 \pm 14$, $\Delta\delta = -229 \pm 20$. The isotropic ^{31}P chemical shifts from this study (Tables 5 and 6) are also very similar to those for the corresponding bands in the ^{31}P spectra of the ceramics.^{1,2}

Conclusions

The ^{31}P NMR data are consistent with three distinct phosphorus sites present in the structure of $\text{CaNa}_4(\text{P}_3\text{O}_9)_2$. This is also consistent with the assignment of the centrosymmetric space group $C2/c$ rather than the non-centrosymmetric Cc , the latter would possess six crystallographically distinct phosphorus sites and would be expected to yield a ^{31}P NMR spectrum with six distinct, equally intense resonances. $(\text{NH}_4)_2\text{Na}_2\text{Hg}(\text{P}_3\text{O}_9)_2$ which is essentially isostructural,¹⁶ shows disorder of the Na and Hg sites with site sharing of the 4e and the 8f cation sites. There is no evidence in the crystallographic data of similar disorder in $\text{CaNa}_4(\text{P}_3\text{O}_9)_2$, although this might be difficult to detect by crystallography alone. More convincingly, the ^{23}Na NMR data suggest that only two distinct sodium sites are present in the structure and hence appear to confirm that site sharing does not occur in $\text{CaNa}_4(\text{P}_3\text{O}_9)_2$.

The main conclusion from the analysis of the ^{23}Na and ^{31}P MAS NMR spectra is that the data for $\text{CaNa}_4(\text{P}_3\text{O}_9)_2$ agree very closely with the corresponding data obtained for the Na/Ca/Al/phosphate ceramics¹ and the Na/Ca/phosphate ceramics² and provide compelling evidence that the principal phosphate species in those ceramics is indeed the cyclic triphosphate as was proposed.

Acknowledgements

We are indebted to Miss T. Di Cristina for help in the chemical analysis of the sample. Two of us (T. N. and I. A.) wish to thank NATO for funding a Collaborative Research Grant. We also wish to thank the University of London Intercollegiate Research Service in High Field NMR at QM for the provision of the Bruker AMX-600 NMR spectrometer and the Daresbury Laboratory UK, for access to synchrotron radiation facilities and use of the ICSD database.

References and notes

- I. Abrahams, K. Franks, G. E. Hawkes, G. Philippou, J. Knowles, P. Bodart and T. Nunes, *J. Mater. Chem.*, 1997, **7**, 1573.
- I. Abrahams, G. E. Hawkes and J. Knowles, *J. Chem. Soc., Dalton Trans.*, 1997, 1483.
- J.-C. Grenier, C. Martin and A. Durif, *Bull. Soc. Fr. Mineral. Cristallogr.*, 1970, **93**, 52.
- I. Abrahams, A. Ahmed, G. E. Hawkes, T. Di Cristina and G. Ivanova, in preparation.
- E. J. Griffith, *Inorg. Chem.*, 1962, **1**, 962.

- 6 Programs for Crystal Structure Analysis, Release (97-2), G. M. Sheldrick, Institut für Anorganische Chemie der Universität, Tammanstrasse 4, D-3400 Göttingen, Germany, 1998; G. M. Sheldrick, *Acta Crystallogr., Sect. A*, 1990, **46**, 467; G. M. Sheldrick, SHELXL-93, University of Göttingen, 1993.
- 7 N. Walker and D. Stuart, *Acta Crystallogr., Sect. A*, 1983, **39**, 158.
- 8 ORTEP-3 for Windows: L. J. Farrugia, *J. Appl. Crystallogr.*, 1997, **30**, 565.
- 9 L. J. Farrugia WinGX — A Windows Program for Crystal Structure Analysis, University of Glasgow, 1998.
- 10 A. C. Larson, R. B. Von Dreele and M. Lujan Jr., GSAS, Generalised Structure Analysis System, Neutron Scattering Centre, Los Alamos National Laboratory, California, 1990.
- 11 J. P. Amoureux, C. Fernandez, L. Carpentier and E. Cochon, *Phys. Status Solidi A*, 1992, **132**, 461.
- 12 Bruker WINFIT Program, Bruker Report 1994, vol. **140**, p. 43; WINFIT, Bruker-Franzen Analytik GmbH, 1995.
- 13 WIN-MAS, Bruker-Franzen Analytik GmbH, 1995.
- 14 N. Binstead, J. W. Campbell, S. J. Gurman and P. C. Stephenson, SERC, Daresbury Program Library, Daresbury Laboratory, Warrington, Cheshire, UK, 1992.
- 15 *International Tables for X-ray Crystallography*, eds. C. H. Macgillivray and G. D. Rick, IUCR, Kynoch Press, Birmingham, UK, 1962, vol. III.
- 16 M. T. Averbuch-Pouchot and A. Durif, *Acta Crystallogr., Sect. C*, 1986, **42**, 932.
- 17 ICSD-Inorganic Crystal Structure Data Release 9301, University of Bonn and Gmelin Institute, 1993.
- 18 I. Abrahams and J. C. Knowles, *J. Mater. Chem.*, 1994, **4**, 185; I. Abrahams and J. C. Knowles, *J. Mater. Chem.*, 1994, **4**, 775.
- 19 M. Bagieu-Beucher, I. Tordjman and A. Durif, *Rev. Chim. Miner.*, 1971, **8**, 753.
- 20 H. Y. P. Hong, *Acta Crystallogr., Sect. B*, 1974, **30**, 1857.
- 21 H. Koller, G. Engelhardt, A. P. M. Kentgens and J. Sauer, *J. Phys. Chem.*, 1994, **98**, 1544.
- 22 These ²³Na chemical shifts have been corrected for the change in chemical shift reference material from NaCl solid used by Koller *et al.*²¹ to NaCl solution as described by R. K. Harris and G. J. Nesbitt, *J. Magn. Reson.*, 1988, **78**, 245.
- 23 I. D. Brown and D. Altermatt, *Acta Cryst.*, 1985, **B41**, 244.
- 24 H. M. Ondik, *Acta Crystallogr.*, 1965, **18**, 226.
- 25 In an important earlier report on the ³¹P MAS NMR spectra of crystalline inorganic phosphates (S. Prabhakar, K. J. Rao and C. N. R. Rao, *Chem. Phys. Lett.*, 1987, **139**, 96) it was reported that the number of observed signals from meta- and pyro-phosphates could outnumber the crystallographically distinguishable phosphorus sites. It is possible that the increased number of phosphorus signals was simply the result of scalar ³¹P–³¹P coupling giving ³¹P multiplets but with unexpected intensity distributions.
- 26 M. M. Crutchfield, C. F. Callis, R. R. Irani and G. C. Roth, *Inorg. Chem.*, 1962, **1**, 813.
- 27 M. Cohn and T. R. Hughes, *J. Biol. Chem.*, 1960, **235**, 3250.
- 28 T. Nakai and C. A. McDowell, *Mol. Phys.*, 1992, **77**, 569.
- 29 G. Wu, B. Q. Sun, R. E. Wasylshen and R. G. Griffin, *J. Magn. Reson.*, 1997, **124**, 366.
- 30 S. Dusold, W. Milius and A. Sebald, *J. Magn. Reson.*, 1998, **135**, 500.
- 31 J. Herzfeld and A. E. Berger, *J. Chem. Phys.*, 1980, **73**, 6021.
- 32 U. Haeberlen, *High Resolution NMR in Solids – Selective Averaging*, Academic Press, New York, 1976, p. 9.